MODELLING AND VALIDATION OF THE FORMATION AND OXIDATION OF CENOSPHERES IN A CONFINED SPRAY FLAME

J. YUAN[1], V. SEMIÃO[*,2], AND M. G. CARVALHO[3]

Departamento de Engenharia Mecânica, Instituto Superior Técnico, Av. Rovisco Pais, 1096 Lisboa Codex, Portugal

SUMMARY

Oil combustion generated particulates are mainly soot formed during gas-phase reactions and cenospheres, consisting of ash and unburnt carbon, formed by the liquid-phase pyrolysis. Both kinds of particulates may lead to fouling, augment emissions and change the heat transfer process inside industrial furnaces. In this work, a model to predict the formation, oxidation and spatial distribution of cenospheres is presented and it is developed based on experimental results and on the governing physical mechanisms. This model was coupled to the standard dual eulerian–lagrangian framework to predict two-phase flows combustion. The gas-phase combustion-related properties are calculated by means of time-averaged eulerian conservation equations, in addition to the k–ε turbulence model. The droplets and cenospheres balance equations are solved in a lagrangian fashion, with a stochastic approach to turbulent dispersion. The gaseous turbulent-diffusion flame is modelled using a clipped-Gaussian pdf to account for fluctuations of scalar properties. Chemistry is assumed to be fast. Radiation is modelled by the discrete transfer method. In order to validate the model, the whole procedure was applied to the prediction of a cylindrical laboratory furnace, oil-fired by an industrial-type burner, where experimental data are available. The comparison of predictions against experimental values showed good agreement and, therefore, the validity of the model. The study has proved that the reduction of particulate emissions is achievable through control of aerodynamics, combustion and the quality of atomization. © 1997 by John Wiley & Sons, Ltd.

1. INTRODUCTION

1.1. Preamble

Combustion and pollution have been somewhat synonymous topics since mankind's discovery of fire. As a result of concerted, world-wide concern over the past two decades, for what is being emitted to the environment via the smokestack and the tail pipe, great strides have been made towards burning fuels cleanly. The steadily increasing severity of emissions regulations has been leading to much research on the mechanisms of pollutants formation. In addition, the awareness of the limitation of energy resources and the increase of fuel prices promoted an increase in the consumption of residual fuel-oils and a considerable interest from industrial intensive energy users to support the construction of mathematical models which reliably simulate the performance of combustors. The simulation of oil combustion poses many problems and requires reliable models of the complex processes of soot and cenosphere formation and destruction.

[1]Visiting Professor
[2]Assistant Professor
[3]Full Professor
*Correspondence to V. Semião, Departamento de Engenharia Mecânica, Instituto Superior Técnico, Av. Rovisco Pais, 1096 Lisboa Codex, Portugal. e-mail: viriato@navier.ist.utl.pt

Fouling within industrial furnaces is a relatively recent research subject, due to its noxious nature and its interference in the combustion process. In oil-fired combustion chambers fouling can interact with the efficiency of the process, as the sets of deposition mechanisms, active at high-temperature regimes, can significantly affect the heat transfer process. Indeed, the particulate formed during oil combustion produce deposits on the walls, which reduce heat transfer, and so influence the combustion reactions. Prediction codes capable of computing the aerodynamics, mixing, combustion and thermal radiation in industrial combustors to a reasonable degree of accuracy exist. However, these predictive tools have been far from sufficiently employed as a means of permitting both the knowledge of particulate distribution inside furnaces and the emissions reduction control to be applied directly in the quest for improved burner and combustor designs. The control of fouling inside combustion chambers is probably achievable through the improvement of quality of atomization, combustion parameters and, to some extent, through optimization of the general operating conditions; but parametric trials on full scale equipment are very expensive and accurate measurements are difficult. The number, and so the cost, of trials required to be performed could be considerably reduced with the aid of reliable physical and mathematical modelling.

The present paper describes the physical and mathematical modelling of an oil-fired, axially symmetric laboratory furnace. The turbulence, gaseous combustion, liquid-phase lagrangian tracking and radiation models are those used previously by Barreiros *et al.* (1993) to predict the same furnace. The present work, however, extends the previous work to the calculations of particulate trajectories, with sub-models for its formation and oxidation rates, and the results are validated against existing experimental data. In order to study the model sensitivity and to evaluate the influence on particulate emissions of changes in operating conditions such as swirl number, excess air level and atomization quality, a parametric study was carried out and the results are compared with experimental data.

1.2. *Particulate formation and oxidation mechanisms*

According to the phase where particulate precursor reactions occur, oil combustion can lead to the formation of two distinct kinds of solid particles. Soot is formed during reactions of the gaseous phase and usually exhibit sizes below one micron. Conversely, coke particles are the result of the liquid-phase pyrolysis of the heavy fuel-oil droplets, in the last stage of their vaporization history, e.g. Lightman and Street (1983). Moreover, cenospheres are larger in size — typical values of coke particle sizes are, according to Marrone *et al.* (1984), within the range of $1-50~\mu m$ and sometimes even exhibiting a few hundred microns, e.g. Bomo *et al.* (1984). The pyrolysis of large hydrocarbon molecules leads to formation of carbonaceous solid shells containing several blowholes, as a result of the volatiles migration. It is within these hard cenospheres that fuel impurities concentrate. The fraction of fuel-oil converted to these cenospheres appears to be solely dependent on the composition of the original fuel-oil–Marrone *et al.* (1984). In their experiments with single droplets of heavy fuel-oil, Urban and Dryer (1990a, b) and Urban *et al.* (1992) found that each droplet forms a cenosphere. Furthermore, they found that the mass fraction of the initial oil droplet converted to coke is determined by the Coke Formation Index (CFI), in turn constant for any given fuel over a wide range of combustion conditions. Therefore, the size of a cenosphere depends on the fuel properties and on the initial diameter of the precursor oil droplet. This fact was corroborated by the experimental work of Ballester and Dopazo (1994), where the authors found that the ratio between the values of the initial diameter of a droplet and the size of the originated cenosphere is constant.

The physical mechanisms for coke particles oxidation have also been experimentally studied by Urban and Dryer (1990a, b) and Urban *et al.* (1992). In those works, the authors found that the initial diameter of the recently formed cenospheres keeps almost constant throughout their life history, in spite of the subsequent oxidation process. This oxidation process appears to occur mostly on the inner surface of the cenosphere porous structure. Furthermore, the heterogeneous combustion of cenospheres is controlled by their porosity and size, by their temperature history and by the local gaseous oxygen concentration. Consequently, besides

the dependence on fuel properties, particulate emissions are also dependent on the quality of atomization and on the combustion conditions.

It can be seen that many researchers (e.g., Lightman and Street, 1983; Marrone *et al.*, 1984; Urban and Dryer, 1990a, b; Clayton and Back, 1989) have experimentally studied the physical mechanisms for coke particles formation and oxidation in oil combustion. However, these experimental results are far from being extensively used and applied to numerical modelling of particulate emissions from industrial furnaces. The work of Byrnes *et al.* (1996) is an exception.

The effect on fouling, heat transfer and emissions are, to a great extent, determined by particulate formation and oxidation processes and by its spatial distribution inside the furnace. Therefore, the correct quantification of the above-mentioned physical processes requires the knowledge of the spatial distribution of particulates within oil-fired combustion chambers. Moreover, the control and reduction of particulate emissions are achievable through the improvement of the combustion conditions, a task that can be carried out economically by the use of numerical methods. For this purpose, physical models for coke particulate formation and oxidation in oil-fired combustors, based on the above-mentioned experimental results are presented herein.

2. MATHEMATICAL AND PHYSICAL MODELLING

2.1. Basic transport equations and physical modelling for oil combustion

The mass, momentum, energy, and chemical species eulerian transport equations for a two-dimensional turbulent reacting flow are applied in their cylindrical co-ordinate form. The two-equation turbulence model of Launder and Spalding (1972), in which equations for the turbulent kinetic energy k and its dissipation rate ε are solved, was used. The combustion model was based on the idea of a single step and fast reaction between the oxidant and the gaseous fuel—vaporized at the droplet surface and diffused to the flame front—assumed to combine in stoichiometric proportion. It was also assumed that all species and heat diffuse at the same rate, and hence the instantaneous gas composition can be determined as a function of a conserved scalar variable, e.g. Williams and Libby (1980). Any conserved scalar may be chosen and here the mixture fraction f, defined as the mass of fuel present, both burnt and unburnt, was used.

In a turbulent flow, the mixture fraction will fluctuate and knowledge of its mean value is insufficient to allow the determination of the mean values of such quantities as density and temperature because of the nonlinearity of the relationships. A statistical approach to describe the temporal nature of the mixture fraction fluctuations was adopted. The time-averaged value of any property ϕ solely dependent on f can then be determined from the convolution of ϕ with the pdf. The clipped-Gaussian pdf of Lockwood and Naguib (1975) for the mixture fraction, which is completely defined by its mean value f, and variance g, was employed. The variables, f and g, also obey modelled transport equations.

The discrete transfer radiation prediction procedure of Lockwood and Shah (1981) was utilized in this study. This procedure is numerically exact and applicable to arbitrary geometries. It is based on the solution of the fundamental radiative transfer equation within discretized solid angles. The last feature is of particular importance in the real world of geometrically intricate combustion chambers. The gas absorption coefficient was calculated from the two-grey-plus-a-clear-gas fit of Truelove (1981). The optical behaviour of the soot was accommodated by discretizing the soot absorption coefficient such that it is uniform at empirically determined values within each of the bands of the mentioned model.

The governing equations of an axisymmetric two-phase turbulent reacting flow, with swirl, can be written in a general form:

$$\frac{\partial}{\partial x}(\rho u \Phi) + \frac{1}{r}\frac{\partial}{\partial r}(\rho r v \Phi) = \frac{\partial}{\partial x}\left(\Gamma_\Phi \frac{\partial \Phi}{\partial x}\right) + \frac{1}{r}\frac{\partial}{\partial r}\left(r\Gamma_\Phi \frac{\partial \Phi}{\partial r}\right) + S_\Phi + S_{\Phi,\mathrm{d}} \qquad (1)$$

Table 1. The source terms S_Φ and $S_{\Phi,\mathrm{d}}$ for different Φ variables of equation (1)

Variable Φ	S_Φ	$S_{\Phi,\mathrm{d}}$
1 (continuity equation)	0	$-\displaystyle\sum_{\text{droplets}} (m_{\mathrm{d},t+\delta t} - m_{\mathrm{d},t})$
u	$-\dfrac{\partial p}{\partial x} + \dfrac{1}{r}\dfrac{\partial}{\partial r}\left(r\mu_{\text{eff}}\dfrac{\partial v}{\partial x}\right) + \dfrac{\partial}{\partial x}\left(\mu_{\text{eff}}\dfrac{\partial u}{\partial x}\right)$	$-\displaystyle\sum_{\text{droplets}} (m_{\mathrm{d},t+\delta t}u_{\mathrm{d},t+\delta t} - m_{\mathrm{d},t}u_{\mathrm{d},t})$
v	$-\dfrac{\partial p}{\partial r} + \dfrac{1}{r}\dfrac{\partial}{\partial r}\left(r\mu_{\text{eff}}\dfrac{\partial v}{\partial r}\right) + \dfrac{\partial}{\partial x}\left(\mu_{\text{eff}}\dfrac{\partial u}{\partial r}\right)$ $-\dfrac{2\mu_{\text{eff}}v}{r^2} + \dfrac{\rho w^2}{r}$	$-\displaystyle\sum_{\text{droplets}} (m_{\mathrm{d},t+\delta t}v_{\mathrm{d},t+\delta t} - m_{\mathrm{d},t}v_{\mathrm{d},t})$
w	$-\dfrac{\rho v w}{r} - \dfrac{1}{r}\dfrac{\partial}{\partial r}(\mu_{\text{eff}}w) + \mu_{\text{eff}}\dfrac{\partial(w/r)}{\partial r}$	$-\displaystyle\sum_{\text{droplets}} (m_{\mathrm{d},t+\delta t}w_{\mathrm{d},t+\delta t} - m_{\mathrm{d},t}w_{\mathrm{d},t})$
k	$G_k - C_{\mathrm{D}}\rho\varepsilon$	0
ε	$\dfrac{C_1\varepsilon G_k - C_2\rho\varepsilon^2}{k}$	0
f	0	$-\displaystyle\sum_{\text{droplets}} (m_{\mathrm{d},t+\delta t}f_{\mathrm{d},t+\delta t} - m_{\mathrm{d},t}f_{\mathrm{d},t})$
g	$C_{\mathrm{g}1}G_{\mathrm{g}} - C_{\mathrm{g}2}\rho\dfrac{\varepsilon}{k}g$	0
h	$S_{\text{rad}} = \displaystyle\sum_{\text{rays}} (I_{n+1} - I_n)\,\Omega\,\mathrm{d}\Omega\,\mathrm{d}A$	$-\displaystyle\sum_{\text{droplets}} (m_{\mathrm{d},t+\delta t} - m_{\mathrm{d},t})(h_{\text{fu}} - L_{\text{fu}})$

Note: $\mu_{\text{eff}} = \mu + \mu_t$, $\mu_t = \rho C_\mu k^2/\varepsilon$, $G_{\mathrm{g}} = 2\mu_t\left[\left(\dfrac{\partial f}{\partial x}\right)^2 + \left(\dfrac{\partial f}{\partial r}\right)^2\right]$,

$$G_k = \mu_t\left\{2\left[\left(\frac{\partial u}{\partial x}\right)^2 + \left(\frac{\partial v}{\partial r}\right)^2 + \left(\frac{v}{r}\right)^2\right] + \left(\frac{\partial u}{\partial r} + \frac{\partial v}{\partial x}\right)^2 + \left(\frac{\partial w}{\partial x}\right)^2 + \left(\frac{\partial w}{\partial r} - \frac{w}{r}\right)^2\right\}$$

where S_Φ is the source term of the transport equation and $S_{\Phi,\mathrm{d}}$ is an additional source term representing the interaction between different phases. The corresponding values of Φ, S_Φ and $S_{\Phi,\mathrm{d}}$ are indicated in Table 1. The quantities $C_{\mathrm{D}}, C_\mu, C_1, C_2, C_{\mathrm{g}1}, C_{\mathrm{g}2}$ appearing in Table 1 are standard constants of the k–ε turbulence model and of the combustion model (see, e.g. Launder and Spalding, 1972; Lockwood and Naguib, 1975), and are used in these predictions.

For the liquid-phase modelling it was assumed that a finite number of droplet size ranges represent the continuous size distribution of the actual spray. The momentum and thermal balance equations for the droplets were solved in a lagrangian fashion with a stochastic treatment for turbulent dispersion.

A two-stage droplet life history was assumed for the oil droplet vaporization: heat up to the boiling temperature with no evaporation followed by heat transfer controlled vaporization, e.g. Abbas and Lockwood (1985). The rate of change of the droplet temperature T_{D} is computed from its energy balance:

$$\frac{\mathrm{d}T_{\mathrm{D}}}{\mathrm{d}t} = \frac{6K_{\mathrm{g}}\mathrm{Nu}}{\rho_{\mathrm{D}}C_{p,\mathrm{D}}D_{\mathrm{D}}^2}(T_{\mathrm{g}} - T_{\mathrm{D}}) + \frac{3L}{C_{p,\mathrm{D}}D_{\mathrm{D}}}\frac{\mathrm{d}D_{\mathrm{D}}}{\mathrm{d}t} \tag{2}$$

where D_{D} is the droplet diameter, K_{g} is the gas thermal conductivity, ρ_{D} and $C_{p,\mathrm{D}}$ are the density and specific heat of the droplet, L is the latent heat of vaporization and T_{g} is the local gas temperature.

In equation (2), Nu stands for the Nusselt number given by

$$Nu = 2.0 + 0.55 Re_D^{1/2} Pr^{1/3} \tag{3}$$

where Pr is the Prandtl number and Re_D is the droplet Reynolds number defined as in the work of Abbas and Lockwood (1985).

The rate of droplet diameter diminution is given by

$$\frac{dD_D}{dt} = - \frac{4CK_g}{\rho_D C_{p,g} D_D} \ln(1 + B) \tag{4}$$

where $C_{p,g}$ is the gas specific heat. The transfer number B, obeys the relation

$$B = \frac{C_{p,g}}{L}(T_g - T_D) \tag{5}$$

where C is an empirical correction factor to account for the effect of convection on the evaporation rate, given by Faeth (1987):

$$C = 1 + \frac{0.278(Re_D^{1/2} Pr^{1/3})}{(1 + 1.237/Re_D Pr^{4/3})^{1/2}} \tag{6}$$

As soot is formed in gas-phase reactions, an eulerian approach was used and the transport equation for the soot mass fraction was built. The simple global model, established by Khan and Greeves (1974), was used to calculate the source term for the soot production rate:

$$S_f = C_f p_f \phi^n \exp(-E/RT_g) \tag{7}$$

where p_f, ϕ, R, E and T_g are, respectively, the fuel partial pressure, the equivalence ratio, the universal gas constant, the activation energy and the local gas temperature, and C_f and n are constants obtained from Abbas and Lockwood (1985). Since p_f, ϕ, and T_g may be related to mixture fraction, the mean value of the source term is computed from the convolution:

$$\bar{S}_f = \int_0^1 S_f p(f) \, df \tag{8}$$

where $p(f)$ is the mixture fraction pdf.

Soot production is essentially zero for equivalence ratios ϕ, less than the incipient sooting limit (see Glassman and Yaccarino, 1981) and for ϕ in excess of a value corresponding roughly to the upper flammability limit.

A simple model for estimating the soot oxidation rate (Magnussen and Hjertager, 1977) was adopted. Following conventional turbulence concepts, the model presumes that turbulence decay of the mixing rate is proportional to the magnitude of the time-mean soot mass concentration m_s, and to the time scale of the large-scale turbulence motion ε/k. Depending on the oxygen concentration the overall soot burning rate, to be included in the source term of its transport equation, is given by

$$S_d = A m_s \rho \frac{\varepsilon}{k} \min\left(1, \frac{m_{ox}}{m_s s_s + m_f s_f}\right) \tag{9}$$

where A is the model constant, m_{ox} and m_f are the local mean oxygen and fuel concentrations, and s_s and s_f are the stoichiometric soot and fuel oxygen requirements. The details of the model can be found in the work of Coelho and Carvalho (1995).

2.2. Coke formation and oxidation modelling

Urban and Dryer (1990a, b), Urban et al. (1992) and Ballester and Dopazo (1994) have studied extensively the cenospheres formation during the combustion of heavy fuel-oil sprays. In their experiments, each and every droplet with an initial diameter in the range 200–700 μm was found to form a cenosphere. Additionally, it was established in their work that the mass fraction of the initial fuel droplet converted to coke, the coke Formation Index (CFI) was constant for any given fuel over a wide range of combustion conditions. CFI is defined by

$$\text{CFI} = 6\,\frac{D_c^2}{D_o^3}\,\frac{\rho_c\tau}{\rho_o} \tag{10}$$

where subscripts c and o refer to the coke particulate and oil droplet, respectively. D is the outside diameter, ρ is the density and τ is the thickness of the particle shell.

From the work of Urban et al. (1992) it was found that CFI, that can be taken as the coke formation potential of residual fuel-oils, is constant. Moreover, the product $\rho_c\tau$ was also found to be constant for a given fuel-oil. Therefore, the ratio of particulate diameter to droplet diameter is constant over a wide range of initial droplet sizes. Considering the results of the above-mentioned experiments, it was assumed in this work that a cenosphere forms at the last stage of the droplet vaporization, when its diameter reaches the critical value determined by the value of CFI. The recently formed cenosphere itself undergoes an oxidation process, with constant diameter and decreasing density.

It should be noted that the experiments of Urban and Dryer (1990a, b) and Urban et al. (1992) were carried out for oil droplets with initial diameter values in the range 200–700 μm. However, for energetic efficiency reasons, in most practical cases (including the case here) the initial droplet diameters of most combusting sprays are lower than 200 μm. As far as the extension of their results to smaller droplet sizes is concerned, Urban and Dryer (1990a, b) and Urban et al. (1992) believed that the value of CFI should remain constant and unchanged even for droplet sizes smaller than 200 μm. However, the thin cenosphere shell model would become increasingly less accurate with the decrease of the initial droplet diameter, and a uniform density model would be more appropriate — e.g. Urban et al. (1992). Therefore, the uniform density model was adopted in the present work.

The coke oxidation was modelled assuming that a surface reaction producing CO occurs, being CO subsequently oxidized to CO_2 in the gas phase. The rate of oxidation is controlled by the oxygen diffusion rate to the particle surface and by the chemical reaction rate. Following Smith (1983), an apparent order of $\frac{1}{2}$ for the oxygen molar concentration was assumed leading to the following rate of carbon consumption:

$$\frac{dm_c}{dt} = -\frac{k_c}{2k_D}\left[-k_c + (k_c^2 + 4k_D^4 m_{O_2})^{1/2}\right] \tag{11}$$

the diffusion rate k_D being given by

$$k_D = \frac{4m_c D_{O_2}}{D_D} \tag{12}$$

where m_c and m_{O_2} are the molar masses of carbon and oxygen, and D_{O_2} is the binary mass diffusion coefficient of oxygen in the boundary layer. The reaction rate k_c is given by

$$k_c = A_c \exp\left(-\frac{E_c}{RT}\right) \tag{13}$$

where the rate constants determined by Holmes et al. (1990) were used here and have the values: $A_c = 18\ \text{kg m}^{-2}\,\text{s}^{-1}\,(\text{mol m}^{-3})^{-0.5}$ and $E_c = 78\ \text{kJ mol}^{-1}$. In this work, a constant particle diameter during the oxidation phase of the cenospheres was assumed.

3. DESCRIPTION OF THE FURNACE AND OPERATING CONDITIONS

The prediction procedure described above was applied for the solution of the process in an oil-fired, two-dimensional axisymmetric furnace, described by Costa *et al.* (1991a, b), for which experimental data are available. This laboratory furnace is large enough to ensure that the essential physics of full-scale combustors is simulated. In particular, it is large enough to ensure fully turbulent flow combined with significant thermal radiation transfer, but small enough to enable the collection of detailed and reliable in-flame measurements. In addition, its upright cylindrical geometry ensures that the flow is axially symmetrical, allowing economic computer simulation by two-dimensional prediction codes. The combustion chamber is cylindrical in shape. Its axis is vertical to minimize asymmetry due to natural convection and biased particulate deposition and it is down-fired to facilitate particulates removal. The cylinder comprises of ten water-cooled steel segments, each 0·3 in height and 0.6 m in internal diameter. The roof section and the upper four segments are lined with a suitable layer of refractory, which can withstand temperatures up to 1700°C, and a suitable ceramic fibre blanket, sandwiched between the refractory and the water-cooled jacket. Once assembled, the joint between adjacent segments is rendered gas tight with high-temperature gaskets and a refractory sealant.

The near-burner region geometry is sketched in Figure 1 and consists of a burner gun and a secondary air supply in a conventional double-concentric configuration, terminating in an interchangeable castable refractory quarl of variable half-angle and a length-to-diameter ratio of one. The secondary air enters the plenum chamber situated above the burner in which it encounters a moveable block swirl generator. The air then flows through an interchangeable cylindrical duct and subsequently into the refractory quarl section.

The furnace operating conditions and the fuel-oil properties are listed in Table 2. By comparison of these properties with those presented in the work of Urban *et al.* (1992), the CFI was evaluated.

In order to investigate the effect of the quality of atomization on the rate of particulate formation, two different experimental droplet size distributions of sprays, measured by Costa *et al.* (1991a) and depicted in
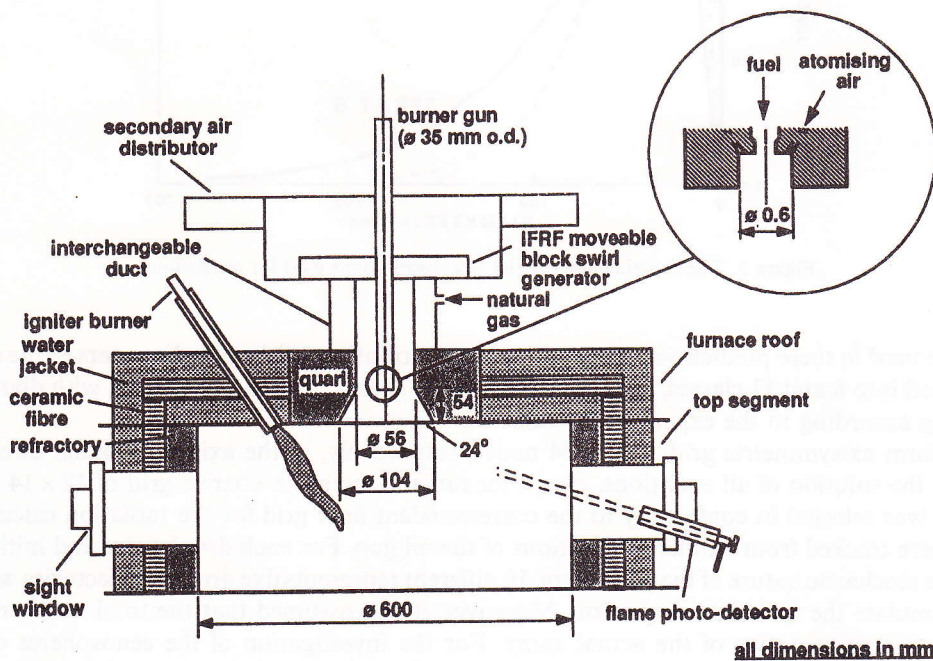

Figure 1. The furnace roof and the near-burner region geometry

Table 2. Fuel properties and furnace operation conditions

Fuel properties		Operation conditions	
Carbon	86·4%	Fuel flow	12 kg h^{-1}
Nitrogen	0·35%	Excess air	0–20%
Hydrogen	9·8%	Secondary air swirl number	0·5–1.3
Sulphur	2·97%	Atomizing air flow	15 kg h^{-1}
Oxygen	0·44%	Secondary air flow	170·2 kg h^{-1}
Ash	0·04%	Fuel temperature	368 K
Gross calorific value	42·5 × 10^6 J kg^{-1}	Atomizing air temperature	293 K
Latent heat	2·73 × 10^5 J kg^{-1}	Secondary air temperature	573 K
Specific heat	2·52 × 10^3 J kg^{-1} K^{-1}		
Density	988 kg m^{-3}		
Viscosity (75°C)	0·112 N s m^{-2}		
Saturation temperature	180°C		
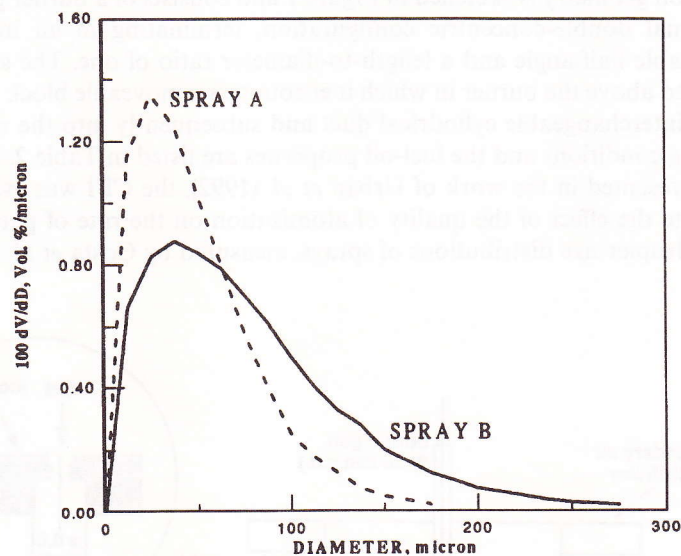
Figure 2. The experimental droplet size distributions used for predictions

Figure 2, were used in these predictions. The continuous distributions of droplet diameters of the inlet sprays were discretized into 8 and 11 classes, respectively, for spray A and spray B of Figure 2, with diameter range values varying according to the experimental values.

A non-uniform axisymmetric grid of 55 × 54 nodes, respectively, in the axial and radial directions, was generated for the solution of all equations, except for radiant energy. A coarser grid of 18 × 14 nodes, also non-uniform, was selected in conformity to the correspondent finer grid for the radiation calculations.

Droplets were tracked from 5 different positions of the oil gun. For each droplet size and initial position, and due to the stochastic nature of the procedure, 10 different representative droplet trajectories were tracked in order to simulate the turbulent dispersion. Moreover, it was assumed that the total number of tracked trajectories was representative of the actual spray. For the investigation of the cenospheres distribution inside the furnace, oil droplets, coke particles and completely burn out ash particulate trajectories were tracked.

Droplets and particulate trajectories were tracked in a lagrangian fashion according to the Newton's law, assuming that the only forces acting on droplets and particulate were the drag force and gravity. The turbulent dispersion model for the discontinuous phase, used in this work, was presented by Dukowicz (1980) and has been extensively applied in spray calculations.

4. RESULTS AND DISCUSSION

4.1. General aerodynamics and flame characteristics

The predicted flow fields for swirl numbers of the secondary air of 0·9 and 0·5 are shown in Figure 3. It can be seen from Figure 3(a) that an intensive and large internal recirculation zone (IRZ) is formed due to the high level of swirl imparted to the secondary air. The atomizing air velocity is 110 m s^{-1}. The IRZ is intensive enough to exert a pulling effect against the atomizing air jet, bending it backwards to the main stream. The external recirculation zone (ERZ), usually appearing in this type of geometry configuration due to the sudden expansion immediately after the quarl, was not detected for this flow condition. However, when the secondary air swirl number was reduced to 0·5, an ERZ was formed. In this case, it must be noted, the axial momentum of the high velocity primary air jet was high enough to prevent the formation of an IRZ.

Figure 4 shows the representative trajectories of two groups of droplets and respective cenospheres subsequently formed, with initial diameters of 50 and 150 μm. The values presented herein are referred to predictions for spray A of Figure 2. Figure 4(a) corresponds to the predictions for the highest value of the secondary air swirl number. This figure shows that, at first, the droplets or the cenospheres reach the IRZ and are then recirculated back into the main stream. Conversely, Figure 4(b) shows that the flow configuration, resulting from the decrease of the secondary air swirl number to 0·5, allows for part of the droplets or cenospheres to fly forward into the axis of the furnace and then to the outlet. However, part of the droplets or cenospheres are recirculated back to the ERZ. The presence of both the IRZ and the ERZ contributes to the improvement of the combustion efficiency as the residence time of droplets or cenospheres is largely increased.

The predicted values for the gas temperature inside the furnace are depicted in Figure 5. The highest temperature is found to occur in a region near the inlet as a result of the high value of the vaporization rate of
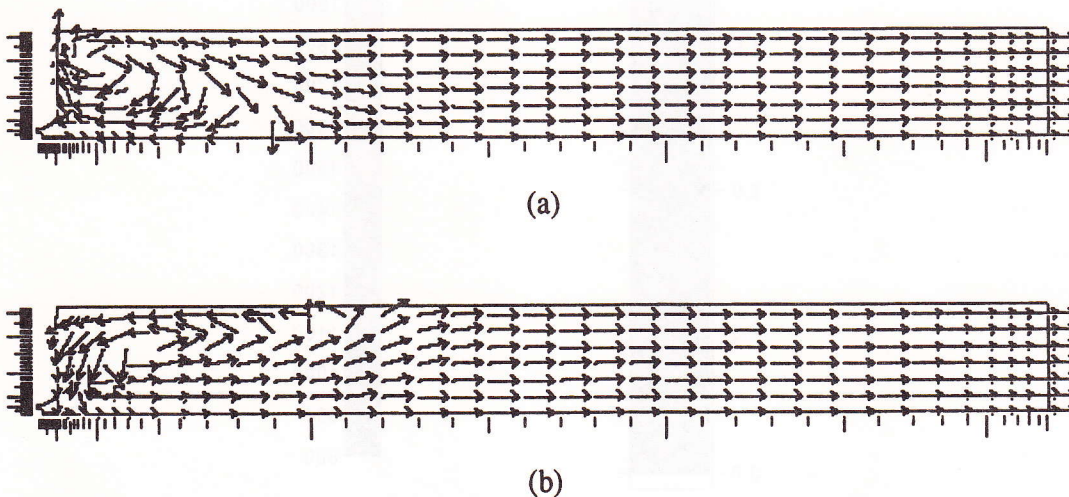

(a)

(b)

Figure 3. The gas flow pattern: (a) secondary air swirl number = 0·9; (b) secondary air swirl number = 0·5
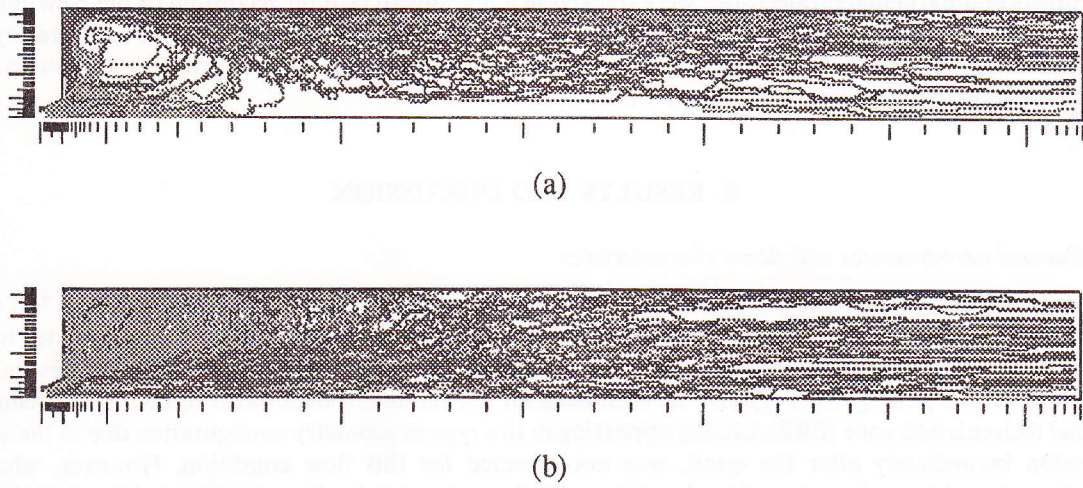
(a)

(b)

Figure 4. The trajectories of oil droplets/cenospheres: (a) secondary air swirl number = 0.9; (b) secondary air swirl number = 0·5
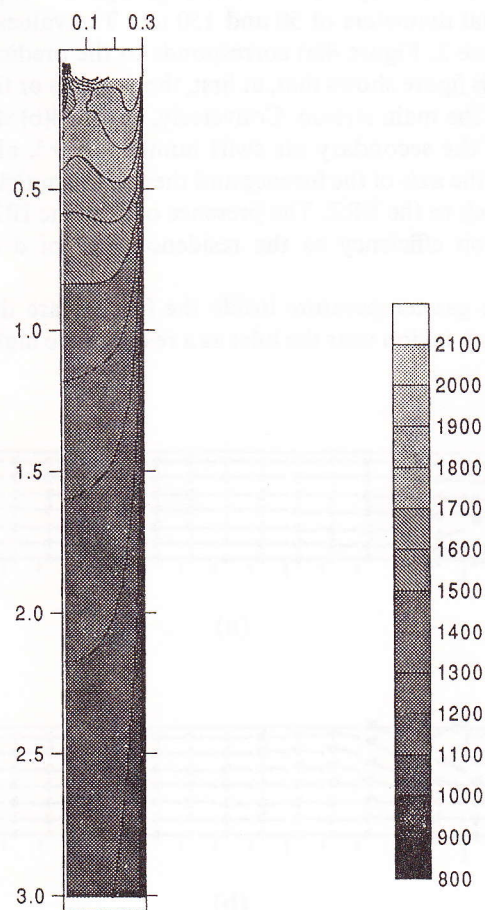

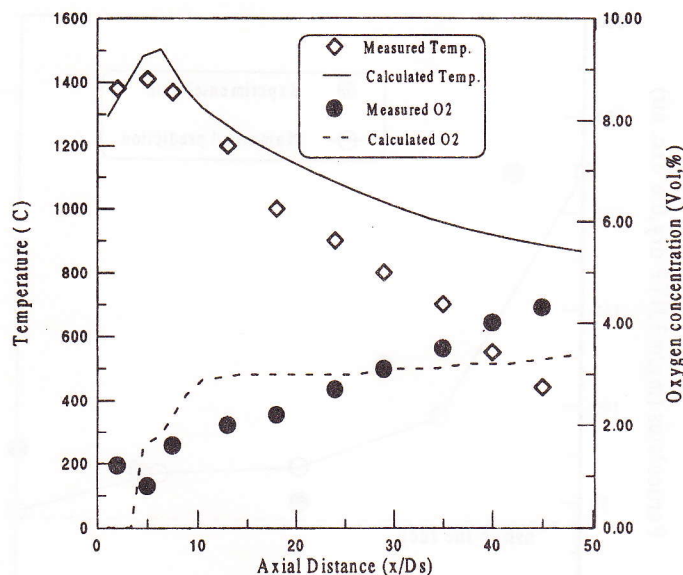Figure 5. The predicted temperature distribution (*K*) inside the furnace

Figure 6. Axial distributions of gas temperature and oxygen concentration

droplets. In Figure 6, the predicted axial values of the gas temperature and oxygen concentration are compared against the corresponding experimental values, obtained by Costa *et al.* (1991b). The trends of both temperature and oxygen concentration are well predicted. However, near the outlet the temperature values are over predicted. This may result from uncertainties in the predictions. Indeed, the lack of experimental data for heat fluxes near the outlet, needed for radiation boundary conditions, may have contributed to the observed discrepancies.

4.2. Particulate formation, oxidation and distribution

Although soot is a kind of particulate formed in oil combustion, and was calculated in this work, its contribution to emissions is insignificant when compared to other types of particulate. This is due to the small amount of fuel-oil that converts to soot and to the very fast oxidation rate of recently formed soot particles under high-temperature environments, as observed in a previous study of Carvalho *et al.* (1996). Soot is mainly of concern because its presence greatly augments the radiation heat transfer. Therefore, the discussion herein will be centred on the processes involving cenospheres. According to the model used herein, cenospheres are formed immediately after the droplets vaporization. Since the initial droplet sizes are small, their vaporization time is drastically short.

A cenosphere consists of ash originally in the fuel-oil and unburnt carbon. The original content of ash in the fuel-oil indicates that its contribution to the particulate emissions is 38 mg m^{-3}. The remainder of those emissions correspond to the unburnt carbon. Parameters such as swirl number, excess air ratio and initial droplet size affect the rate of carbon oxidation and, consequently, the amount of emissions. The study of the influence of such parameters on the amount of particulates leaving the furnace is described below.

Effect of swirl number. The model described herein was applied to the predictions of the furnace described above, for several inlet swirl numbers of the secondary air. The results of particulate concentration at the furnace outlet, as a function of the swirl number, are compared in Figure 7 against the corresponding experimental values, obtained from Barreiros *et al.* (1993). The agreement is reasonable and the trend is well
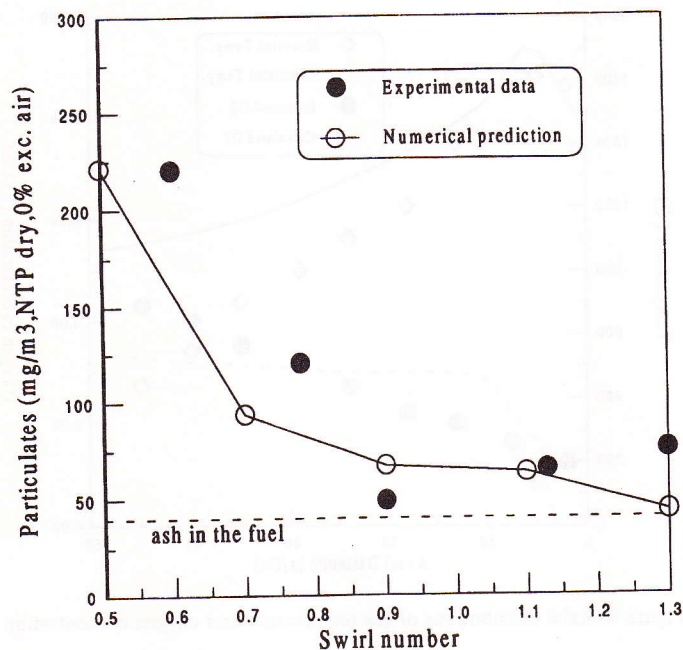
Figure 7. Effect of secondary air swirl number on particulate emissions

predicted. Indeed, the increase of the inlet swirl number leads to an increase of the particles residence time within the furnace due to the appearance and growth of an IRZ and, consequently, the unburnt carbon becomes smaller at the furnace outlet. Moreover, both predictions and experimental data show that for swirl numbers above 0·9 the particulate emissions become almost insensitive to further increase of the swirl number.

Effect of excess air ratio. The model was also applied to a parametric study of the excess air ratio and its influence on the behaviour of the furnace, i.e. as far as particulate emissions are concerned. The results of particulate concentration at the furnace outlet as a function of the excess air value, for an inlet swirl number of 1·2, are compared in Figure 8 against the corresponding experimental values, obtained from Byrnes *et al.* (1996). The trend is well predicted, that is, the excess air has a major influence on the particulate emissions. For excess air values lower than 8%, the diminution of its level leads to a deep increase of the particulate emissions. This is obviously due to the influence of oxygen concentration on the carbon oxidation rate. Indeed, in regions of oxygen deficiency there is an inhibition of the carbon oxidation.

Effect of fuel droplet size distribution. In order to determine the influence of the initial droplet sizes on particulate emissions, two different sprays were used in the predictions–sprays, A and B depicted in Figure 2. Spray A has a higher quality compared to spray B. In the case of the predictions for spray B, the swirl number used was 0·9 and the excess air ratio was 16%. These values led to a particulate concentration value of $161 \, mg \, m^{-3}$ at the outlet. For the same swirl number and excess air ratio, spray A led to a particulate concentration emission value of $67 \, mg \, m^{-3}$ at the outlet. This result is expected because the increase of the initial droplet size leads to the formation of cenospheres with greater diameter. In turn, larger cenospheres take longer to burn out.
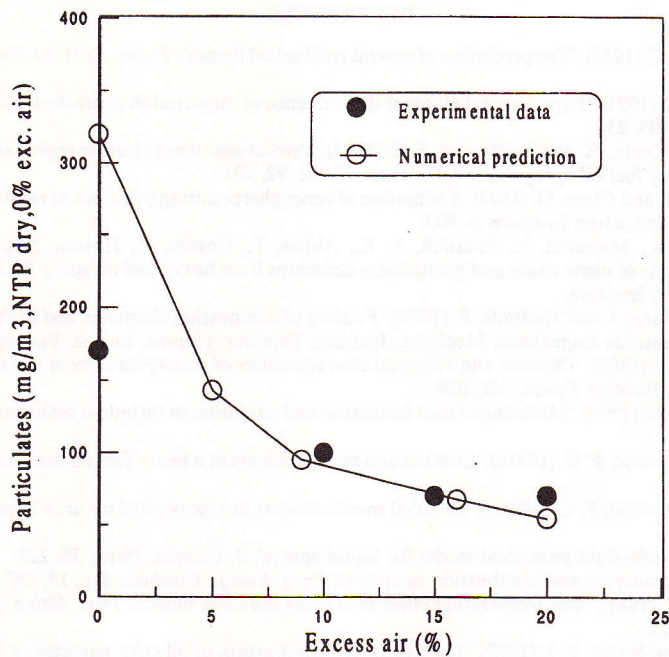
Figure 8. Effect of excess air level on particulate emissions

5. CONCLUDING REMARKS

The present paper described a two-phase flow prediction procedure for the calculation of the combusting flow, heat transfer processes, fouling trends and particulate emissions in oil-fired furnaces. The particulate formed in spray combustion has been identified mainly as soot and cenospheres and may lead to fouling, heat transfer changes, and emissions. In the present work, a model for soot formation and oxidation was selected from the literature and was incorporated in the eularian framework of the global two-phase flow computational procedure. Additionally, a simple model for cenosphere formation and oxidation was developed and is herein validated against experimental data acquired in a two-dimensional laboratory geometry.

Cenospheres are formed from liquid-phase pyrolysis of vaporized droplets and exhibit a relatively fast oxidation rate. The completely or partially burnt out cenospheres are the major cause for fouling and they increase the pollutant emissions. Thus, the numerical characterization of industrial oil-fired furnaces requires the modelling of particulate formation, destruction and spatial distribution together with their influence on the furnace processes.

The physical insight which the present parametric studies have afforded reveals that the particulate emissions can be controlled through careful attention to the residence time of cenospheres inside the furnaces. Indeed, the flow aerodynamics (inlet swirl number) and the combustion conditions (excess air level) may be controlled in order to ensure complete burn-out of carbon. Furthermore, the spray atomization quality is also essential in the particulate emissions, as larger cenospheres take longer to burn out.

ACKNOWLEDGEMENTS

REFERENCES

Abbas, A. S. and Lockwood, F. C. (1985). 'The prediction of several residual oil flames', *Trans. ASME J. Engng Gas Turbines Power*, **107**, 726.

Ballester, J. M. and Dopazo, C. (1994). 'Experimental study of the influence of atomisation characteristics on the combustion of heavy oil', *Combust. Sci. Technol.*, **103**, 235.

Barreiros, A., Carvalho, M. G., Costa, M. and Lockwood, F. C. (1993). 'Predictions of near burner region and measurements of NO_x and particulate emissions in heavy fuel oil spray flames', *Combust. Flame*, **92**, 231.

Bomo, N., Lahaye, J., Prado, G. and Claus, G. (1984). 'Formation of cenospheres during pyrolysis of residual fuel oils', *Proc. 20th Symp. (Int.) on Combustion*, The Combustion Institute, p. 903.

Byrnes, M. A., Foumeny, E. A., Mahmud, T., Sharifah, A. K., Abbas, T., Costen, P., Hassan, S. and Lockwood, F. C. (1996). 'Measurements and predictions of nitric oxide and particulates emissions from heavy fuel oil spray flames', *Proc. 26th Symp. (Int.) on Combustion*, The Combustion Institute.

Carvalho, M. G., Semião, V., Yuan, J. and Andrade, P. (1996). 'Fouling of combustion chambers and high temperature filters', *JOULE Contract Report*, Departamento de Engenharia Mecânica, Instituto Superior Técnico, Lisboa, Portugal.

Clayton, R. M. and Back, L. H. (1989). 'Physical and chemical characteristics of cenospheres from the combustion of heavy fuel oil', *Trans ASME J. Engng Gas Turbines Power*, **111**, 679.

Coelho, P. J. and Carvalho, M. G. (1995). 'Modeling of soot formation and oxidation in turbulent diffusion flames', *J. Thermophys. Heat Transfer*, **9**, 644.

Costa, M., Costen, P. and Lockwood, F. C. (1991a). 'Combustion measurements in a heavy fuel oil fired furnace', *Combust. Sci. Technol.*, **75**, 129.

Costa, M., Costen, P. and Lockwood, F. C. (1991b). 'Detailed measurements in a heavy fuel oil fired large-scale furnace', *Combust. Sci. Technol.*, **77**, 1.

Dukowicz, J. K. (1980). 'A particle–fluid numerical model for liquid sprays', *J. Comput. Phys.*, **35**, 229.

Faeth, G. M. (1987). 'Mixing, transport and combustion in sprays', *Prog. Energy Combust. Sci.*, **13**, 293.

Glassman, I. and Yaccarino, P. (1981). 'The temperature effect in sooting diffusion flames', *Proc. 18th Symp. (Int.) on Combustion*, The Combustion Institute, p. 1175.

Holmes, R., Purvis, M. R. I. and Street, P. J. (1990). 'The kinetics of combustion of oil coke particles', *Combust. Sci. Technol.*, **70**, 135.

Khan, J. H. and Greeves, G. (1974). 'A method for calculating the formation and combustion of soot in diesel engines', *Heat Transfer in Flames*, Afgan and Beér, p. 391.

Launder, B. E. and Spalding, D. B. (1972). *Mathematical Models of Turbulence*. Academic Press, New York.

Lightman, P. and Street, P. J. (1983). 'Single drop behaviour of heavy fuel oils and fuel oil fractions', *J. Inst. Energy*, **56**, 3.

Lockwood, F. C. and Naguib, A. S. (1975). 'The prediction of the fluctuations in the properties of free, round jet, turbulent diffusion flames', *Combust. Flame*, **24**, 109.

Lockwood, F. C. and Shah, N. G. (1981). 'A new radiation solution method for incorporation in general combustion prediction procedures', *Proc. 18th Symp. (Int.) on Combustion*, The Combustion Institute, p. 1405.

Magnussen, B. F. and Hjertager, B. H. (1977). 'On mathematical modelling of turbulent combustion with special emphasis on soot formation and combustion', *Proc. 16th Symp. (Int.) Combustion*, The Combustion Institute, p. 719.

Marrone, N. J., Kennedy, I. M. and Dryer, F. L. (1984). 'Coke formation in the combustion of isolated heavy oil droplets', *Combust. Sci. Technol.*, **36**, 149.

Smith, I. W. (1983). 'The combustion rates of coal chars: a review', *Proc. 19th Symp. (Int.) on Combustion*, The Combustion Institute, p. 1045.

Truelove, J. S. (1981). 'A mixed grey gas model for flame radiation', *AERE Harwell Report No. HL 76/3448/KE*.

Urban, D. L. and Dryer, F. L. (1990a). *Heat Transfer in Combustion Systems*, ASME HTD-Vol 142, Farouk *et al.*, (Eds), p. 83.

Urban, D. L. and Dryer, F. L. (1990b). 'New results of coke formation in the combustion of heavy-fuel droplets', *Proc. 23rd Symp. (Int.) on Combustion*, The Combustion Institute, p. 1437.

Urban, D. L., Huey, S. P. C. and Dryer, F. L. (1992). 'Evaluation of the coke formation potential of residual fuel oils', *Proc. 24th Symp. (Int.) on Combustion*, The Combustion Institute, p. 1357.

Williams, F. A. and Libby, P. A. (1980). 'Some implications of recent theoretical studies in turbulent combustion', *AIAA Paper No. 80-0012*.